DOI: 10.1002/ejic.200600670

$W(CO)_4$(diimine) Structure Revised – Correlating Structure to π* Back-Bonding

Christodoulos Makedonas[a] and Christiana A. Mitsopoulou*[a]

Keywords: Tungsten / Pi interactions / N ligands / Carbonyls / Ligand effects

The bending of axial and equatorial carbonyls, one of the main structural features of the $M(CO)_4$(diimine) compounds (M = Cr, Mo, and W), is elucidated in terms of the π* back-bonding theory by a frontier molecular orbital analysis. Employing $W(CO)_4$(phen) (phen = 1,10-phenanthroline) as a reference compound has proved that the deviation from orthogonality stabilizes the structure by a total amount of 2.95 kJ/mol. Moreover, by an extended comparison of several $W(CO)_4$(diimine) structures, the importance of the magnitude of the binding angle in determining the bonding in these complexes in comparison to the traditional approach of the W–C and C–O bond lengths is underlined. As a result, it is proposed that the correct indices of the extent of back-donation are the deviations of the C–W–C angles from orthogonality and the O–C–W angles from linearity. It is indicated for the first time that the larger the existing deviation the stronger the back-donation. Moreover, a structure-to-properties relation is provided that correlates the bending of the carbonyls to the extent of back-donation. Back-donation is expected to be correlated to the electronic properties of the compounds, such as the extent of solvatochromism.

1. Introduction

The complexes of the type $M(CO)_4$(diimine) (M = Cr, Mo, and W) play an important role in our understanding of the spectroscopic, photophysical, and photochemical behavior of chromophores with low-lying metal-to-ligand (MLCT) charge-transfer excited states.[1–3] These compounds combine an electron-rich, low-valent, typically d^6 metal atom, which is stabilized by the presence of four carbonyl groups along with the good π*-accepting *a*-diimine ligand. The observed lowest lying MLCT state is responsible for several interesting features, such as the negative solvatochromism and the solution luminescence, while it is associated with large, second-order molecular hyperpolarizabilities. This state arises from the transition between a metal/CO localized HOMO–2 and a diimine LUMO (both of b_1 symmetry in the case of the C_{2v} point group).[4,5] Thus the electronic properties of $M(CO)_4$(diimine) make their use quite essential in areas such as the investigation of polymerization processes,[2] the labeling of biomolecules,[6] and the exploitation of solar energy.[7]

All the structures of tetracarbonyl diimine compounds, which are either crystallographically elucidated or theoretically predicted, share two common features. Both of these features are related to the nonorthogonality of the $W(CO)_4$ fragment. More specifically, according to all published structures, the axial carbonyls bend away from the diimine moiety. Moreover, in the majority of the known structures, the two equatorial carbonyl groups bend away from each other. In both cases the linearity of the two CO units is no longer valid.[4–5,8–9] It is also worth mentioning that the M–C–O angle often changes upon electronic excitation.[4] These above-mentioned two features have been observed several times in the past, but they have never been explained in the literature. Herein, these structural characteristics are studied by means of DFT calculations, and our approach is divided into two parts. Firstly, by employing the highly symmetric $W(CO)_4$(phen) complex (phen = 1,10-phenanthroline) we attempted to investigate and discuss their structure from an electronic point of view in terms of the π* back-bonding theory. To proceed with our analysis, we performed a fragments' molecular orbital analysis (FMO) using DFT electron density calculations. Recently, this procedure was successfully used in the case of a related tungsten compound.[5] Secondly, we discussed the same characteristics as they evolved through a series of bidentate N-donor ligands. In the latter case, we succeeded in extracting the structure-to-properties relation (SPR) that governs these compounds.

[a] Inorganic Chemistry Laboratory, Department of Chemistry, National and Kapodistrian University of Athens, Panepistimiopolis, Zografou 15771, Greece
Fax: +30-210-8322828
E-mail: cmitsop@chem.uoa.gr

Supporting information for this article is available on the WWW under http://www.eurjic.org or from the author.

2. Results and Discussion

2.1. Evolution of Back-Donation in $W(CO)_4$(phen)

We started our analysis with $W(CO)_4$(phen) (**1**). Despite this complex being one of the most extensively studied

among compounds of this type it was only recently that Vlček et al. described its electronic ground state and elucidated its emission behavior.[4c,4d] Apart from being easily produced[12] and having an interesting photochemistry it is usually employed for its high symmetry. It belongs to the C_{2v} point group and this makes its structure elucidation, through spectra, significantly easier. Theoretical calculations are also favored for the same reason. In such a molecule, bending of the CO ligands should be clear and free from the difficult to describe nonorthogonal dihedral angles, as in the case of W(CO)$_4$(pq) [pq = 2-(2′-pyridyl)-quinoxaline] where the calculated dihedral angle for N_{py}–N_{qn}–W–C_{ax} is –92.6°.[5]

In the literature, three crystal structures exist as reported in ref.[10a,10c,11] In our case, ground-state calculations have been performed with the aid of Gaussian 98 packages, employing the well-known B3LYP functional, under C_{2v} molecular symmetry. The final structure, obtained by full geometry optimization, is essentially equivalent to the ones that have been previously reported.[4] Nevertheless, there are some differences arising from the comparison with the crystal structure reported in the work of Xiong et al.[11] Specifically, the bending of the two axial carbonyl groups is not identical in the solid phase. This is also depicted by the observed differences in the dihedral angles (78.2 and 151.9° as compared to –103.4 and –177.2° for the dihedral angles O_{ax}–C_{ax}–W–N^1 and O_{ax}–C_{ax}–W–N^2, respectively). These differences are due to the extended hydrogen bonding developed between the oxygen atom of the CO group and a diimine hydrogen atom present in the crystal. Some of the ground-state structural features of the complex that were theoretically derived and experimentally extracted are presented in Table 1. For uniformity purposes the structure under study is the one derived from the calculation.

Table 1. Comparison of selected calculated bond lengths [Å] and angles [°] for **1** with experimental values from X-ray analysis.

C.I.[a]	Exp.[10]	Exp.[11]	Calcd.
W–N	2.239	2.245	2.226
W–C_{ax}	2.011	2.007	2.033
W–C_{eq}	1.968	1.945	1.976
C–O_{ax}	1.140	1.172	1.187
C–O_{eq}	1.147	1.189	1.197
C=N	1.348	1.401	1.384
C=$C^{diim.}$	1.435	1.365	1.433
N–W–N	73.7	73.5	74.2
C_{ax}–W–C_{ax}	172.4	166.2	173.5
C_{eq}–W–C_{eq}	88.7	93.9	92.7

[a] The average value of symmetry related distances or angles is provided.

In order to accomplish the aforementioned task of structure elucidation in terms of back-donation we decided to design a theoretical model. We introduced four theoretical nonexisting structures for the system under study, which represent steps that are equal in number towards orthogonality. Thus, in **1a** the bending of axial oxygen atoms towards one another no longer exists and the W–C–O moiety is linear, while in **1b** the CO groups take up a position along the *x*-axis of the molecule. In **1c**, starting from structure **1**, equatorial oxygen atoms are placed in such a way that the angle W–C–O becomes 180°. Finally, all the above changes are incorporated into structure **1d**. We should underline that all the encountered distances are kept constant. Another constraint, in terms of the selected strategy, is the fixed position of the W–diimine part. By keeping the W–diimine part constant we succeed in revealing the developed electronic forces. Otherwise the system would relax in several directions, leaving the comparison worthless. The above analysis is depicted in Figure 1. The small structural changes that we introduced induce a relative change in the electronic structure of the complex. These changes, along with several electronic characteristics of the five structures, are depicted in Table 2. Frontier molecular orbitals for all the cases are summarized in Table 3.

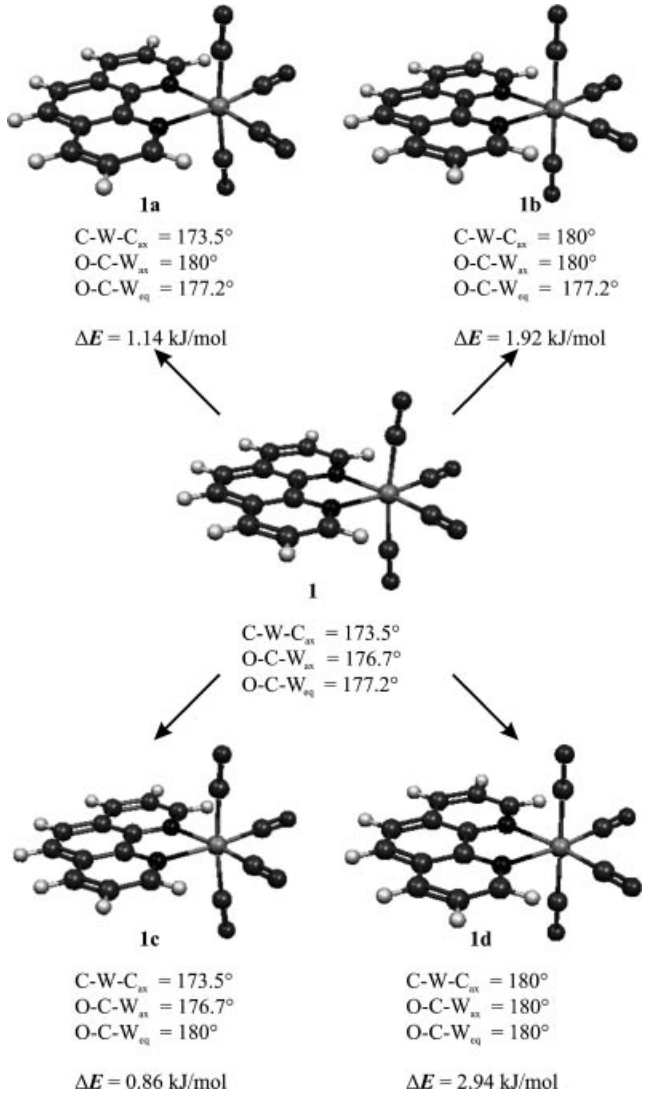

Figure 1. Fragment molecular orbital analysis for **1**.

Before we proceed with our results it is essential to analyze the concepts of donation and back-donation in W(CO)$_4$(diimine) complexes. Bonding in carbonyl compounds is synergic. A carbon σ orbital in CO (the slightly antibonding HOMO) donates electron density to an empty

Table 2. Comparison of selected calculated angles [°] for the ground-state structure of **1** and the hypothetical structures **1a**–**1d**, along with calculated data on electron density donation between the $W(CO)_4$ and the diimine fragments. Data in italics represent the induced changes in **1a**–**1d**.

C.I.	**1**	**1a**	**1b**	**1c**	**1d**
C_{ax}–W–C_{ax}	173.5	173.5	*180*	173.5	*180*
O_{ax}–W–O_{ax}	171.1	*173.5*	*180*	171.1	*180*
C_{eq}–W–C_{eq}	92.7	92.7	92.7	92.7	92.7
O_{eq}–W–O_{eq}	94.8	94.8	94.8	*92.7*	*92.7*
O_{ax}–C_{ax}–W	176.7	*0*	*0*	176.7	*0*
O_{eq}–C_{eq}–W	177.2	177.2	177.2	*180*	*180*
Diim. → W[a]	0.385	0.394	0.398	0.385	0.398
El. repulsion[a]	–0.514	–0.521	–0.522	–0.513	–0.521
H-2 to L[b]	8.0	8.2	7.5	8.1	7.6
b_1 to H-2[c]	6.5[d]	6.7[d]	6.1[d]	6.6[d]	6.2[d]
ΔE[e]	2.36	2.39	2.29	2.35	2.28
ΔE[f]	0	1.14	1.92	0.86	2.95
μ_z[g]	12.86	12.66	12.76	12.93	12.85

[a] Total charge donation and electron repulsion between $W(CO)_4$ and phen fragments. [b] Contribution of the b_1/HOMO–2 (HOMO–1 for **1c**) of the $W(CO)_4$ fragment to the LUMO of the complex. [c] Contribution of the b_1/LUMO of the phen fragment to the HOMO–2 of the complex. [d] In each case there is an additional 1.8% (1.9% for **1a**) contribution from the LUMO+2 of the diimine (also b_1 in symmetry). [e] HOMO–LUMO energy difference in eV. [f] Energy difference between structures, as compared to **1**, in kJ/mol. HOMO–LUMO energy difference in eV. [g] Calculated dipole moment in Debye.

metal orbital of proper symmetry, whereas a filled metal π orbital forms a second dative overlap with an empty CO π orbital. Up to a point, the π-bonding formation strengthens the σ bond and vice versa.

Back-donation also occurs in the case of other π*-accepting ligands, such as 1,10-phenanthroline. On the basis of group theory concepts back-bonding can occur through an overlap with the d_{xz}, d_{xy} and $d_{x^2-y^2}$ metal orbitals, with the latter being more realistically envisioned as a linear combination of d_{z^2}. Under the framework of the above discussion the diimines in the complexes under study certainly act competitively (*trans* influence) with the equatorial carbonyls. Furthermore, the molecules develop their conformation in space in a way that diminishes steric hindrance and electronic repulsion. This electronic repulsion is formed from several interactions among occupied fragment orbitals. $W(CO)_4$(diimine) compounds have a first coordination sphere of octahedral geometry and consequently steric hindrance does not play a significant role in the observed structure. As a result, the interesting structural features that we described seem to arise from a compromise between back-bonding and other electronic repulsions.

According to data presented in Table 3, the three highest occupied molecular orbitals are very close in energy, with the major contributions coming from the d orbitals of the metal and the π* character of the carbonyl group. The high diimine contribution to the HOMO–2 describes the W → diimine π* back-bonding. This energetic similarity holds for all the other complexes of the same type[1] indicating that HOMO–2 is spectroscopically the most important of the

Table 3. Contribution of different fragments to the valence orbitals of the complexes. The HOMO and LUMO are shown in bold.

MO	*E* [eV]	W	phen	CO_{ax}	CO_{eq}
1					
$37a_1$	–1.20	16.2	–2.1	85.8	0.1
$28b_2$	–1.46	20.3	–0.1	70.6	9.2
$15b_1$	–1.57	0.7	97.2	0.8	1.4
$7a_2$	–2.86	0.2	99.1	0.2	0.5
$14b_1$	**–2.93**	**3.8**	**89.8**	**3.1**	**3.4**
$36a_1$	**–5.30**	**64.0**	**0.7**	**0.7**	**34.5**
$6a_2$	–5.58	58.3	3.7	22.8	15.1
$13b_1$	–5.60	54.6	13.7	21.6	10.1
$12b_1$	–7.69	1.5	97.6	0.7	0.2
$5a_2$	–8.00	0.3	99.5	0.1	0.0
$27b_2$	–9.35	0.4	80.0	1.8	17.7
1a					
$37a_1$	–1.19	15.7	–2.3	86.4	0.1
$28b_2$	–1.47	20.4	0.0	70.7	9.0
$15b_1$	–1.56	0.7	97.1	0.7	1.4
$7a_2$	–2.85	0.2	99.1	0.2	0.5
$14b_1$	**–2.92**	**3.9**	**89.6**	**3.1**	**3.4**
$36a_1$	**–5.31**	**64.0**	**0.7**	**0.8**	**34.5**
$13b_1$	–5.59	54.4	14.1	21.7	9.9
$6a_2$	–5.59	58.2	3.7	22.8	15.2
$12b_1$	–7.68	1.5	97.6	0.7	0.2
$5a_2$	–7.98	0.3	99.5	0.1	0.0
$27b_2$	–9.35	0.4	80.4	1.8	17.3
1b					
$37a_1$	–1.27	16.3	–2.3	86.3	–0.3
$28b_2$	–1.51	20.2	–0.1	72.1	7.8
$15b_1$	–1.58	0.9	97.2	0.4	1.5
$7a_2$	–2.86	0.3	99.0	0.2	0.5
$14b_1$	**–2.94**	**3.9**	**90.4**	**2.4**	**3.3**
$36a_1$	**–5.24**	**64.0**	**0.8**	**0.3**	**34.8**
$6a_2$	–5.56	58.8	4.0	22.9	14.3
$13b_1$	–5.62	55.4	13.1	20.5	11.0
$12b_1$	–7.69	1.3	97.6	0.9	0.2
$5a_2$	–8.00	0.3	99.5	0.2	0.0
$27b_2$	–9.35	0.5	79.2	1.8	18.4
1c					
$37a_1$	–1.20	16.4	–2.1	85.7	0.1
$28b_2$	–1.46	20.9	0.0	69.3	9.8
$15b_1$	–1.57	0.7	97.2	0.8	1.3
$7a_2$	–2.86	0.2	99.1	0.2	0.5
$14b_1$	**–2.94**	**3.8**	**89.7**	**3.1**	**3.3**
$36a_1$	**–5.29**	**64.1**	**0.7**	**0.8**	**34.3**
$6a_2$	–5.59	58.4	3.8	22.8	15.1
$13b_1$	–5.59	54.5	13.8	21.6	10.0
$12b_1$	–7.69	1.4	97.7	0.7	0.2
$5a_2$	–8.00	0.3	99.5	0.1	0.0
$27b_2$	–9.36	0.4	80.3	1.8	17.4
1d					
$37a_1$	–1.27	16.4	–2.3	86.2	–0.3
$28b_2$	–1.52	20.8	0.0	70.8	8.4
$15b_1$	–1.58	0.9	97.2	0.4	1.5
$7a_2$	–2.87	0.3	99.0	0.2	0.5
$14b_1$	**–2.95**	**3.9**	**90.3**	**2.4**	**3.3**
$36a_1$	**–5.23**	**64.1**	**0.9**	**0.3**	**34.7**
$6a_2$	–5.56	58.8	4.0	22.9	14.3
$13b_1$	–5.62	55.3	13.2	20.6	11.0
$12b_1$	–7.69	1.3	97.6	0.9	0.2
$5a_2$	–8.01	0.3	99.5	0.2	0.0
$27b_2$	–9.36	0.5	79.4	1.8	18.2

higher occupied orbitals. The main difference between the HOMO and both the HOMO–1 and HOMO–2 is that the character of the carbonyl group is not the same. The HOMO is mainly dominated by the equatorial COs, while HOMO–1 and HOMO–2 are dominated by the axial ones. These three orbitals are related to the t_{2g} orbital set in W(CO)$_6$[13] concerning their π*-back-bonding character. We have to keep in mind that a splitting to a_1, a_2, and b_1 is caused by the C_{2v} symmetry. On the other hand, HOMO–3 to HOMO–5 are localized on the diimine moiety, as well as LUMO, LUMO+1, and LUMO+2, with the first being very close in energy. LUMO+3 and LUMO+4 arise mainly from the axial carbonyls.

The metal d_{xz} contribution to the LUMO and the W/diimine mixing in the HOMO–2 (it contains bonding interactions between the d orbital of the metal and the π* orbitals of the carbonyl groups) are consistent with the π-back-bonding theory. To gain more insight into the bonding scheme of **1** we envisioned the molecule as consisting of two fragments, namely W(CO)$_4$ and phen, acting as a donor and acceptor of electron density, respectively.[14] The derived picture of this fragment orbital analysis is demonstrated in Figure 2 for the HOMO–2 to LUMO. The FMOs of the central unit W(CO)$_4$ are presented on the left side of the diagram, whereas those of the diimine are on the right side. As indicated, the HOMO and HOMO–1 are predominantly localized on the W(CO)$_4$ fragment, with the LUMO being a combination of the LUMO from the diimine and the HOMO–2 from the metal–carbonyls. Of course we have to keep in mind that an increased back-donation of the metal to the heteroligand (N ligand) results in a decreased back-donation to the carbonyl ligands. The aforementioned combination along with the localization of HOMO–2 are indicative of the back-donation procedure. To be more precise, the HOMO–2 of the complex is a mixture of 86.2% of the HOMO–2 of W(CO)$_4$ and 6.5% of the LUMO of phen. This reveals the back-donation path of the electron density from the main core back to the diimine, for a total amount of 0.022 e$^-$, as computed by the Frenking et al.[14] charge decomposition method.

Recently, an analogous treatment of the W(CO)$_4$(pq) complex yielded an amount of 0.054 e$^-$, revealing a more effective back-bonding pathway.[5] At this point we should emphasize that mixing of frontier orbitals is an important parameter of the system and is connected to the negative solvatochromism and the existence of NLO properties for these types of compounds.

According to the aforementioned scheme we could expect the back-donation to the CO groups to be more effective if **1** had not adopted its existing bent geometry. Even if we adopt the atomic angular overlap model it is clear that more electron density is necessary to keep the W(CO)$_4$ fragment together when the structure deviates from orthogonality.

In the current analysis, we examine the bending of the axial carbonyl as a two-step procedure, **1b**→**1a**→**1**. Stated otherwise, we keep the bend of the equatorial CO units towards each other constant and monitor the axial ones

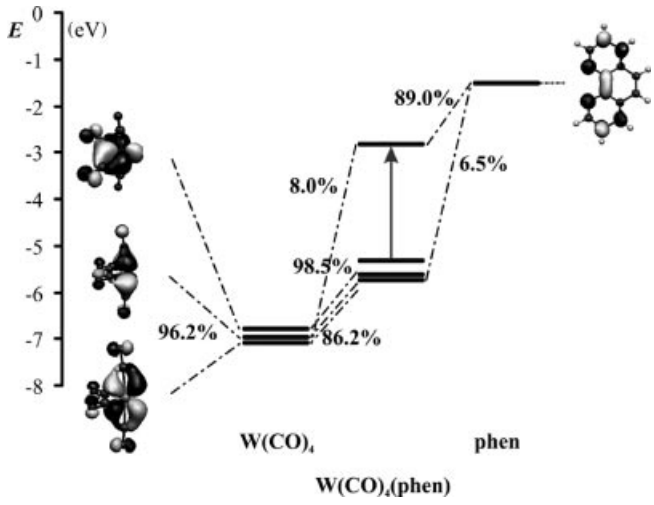

Figure 2. Schematic energy diagram of the induced structural changes in **1**.

deviating from orthogonality. From a frontier orbital point of view, the first step induces major changes, as is expected by the relative geometrical ones. Metal and equatorial carbonyl orbitals are significantly stabilized, while axial carbonyl orbitals seem to become destabilized as well. Diimine orbitals are less destabilised. This finding justifies the inverse order of HOMO–2 (the main, spectroscopically relevant orbital in **1**) and HOMO–1 in **1a**. These trends have an immediate effect on the HOMO–LUMO gap, which according to our calculations increases from 2.30 eV to 2.39 eV in the first step, while it is minimized to 2.37 eV in the second step. This second step is connected to the slight diimine orbital stabilization, whereas the rest of the molecule is destabilized to the same extent. Both steps offer a total 1.92 kJ/mol stabilization to the system. From a partial charges point of view, as calculated by Mulliken's population analysis (provided as Supporting Information), we ascertain that, along the series, the metal and diimine gain electron density at the expense of the carbonyls.

Considering all the aforementioned data, from the back-bonding concept we conclude that the diimine ligation is very crucial. As soon as phenanthroline binds, it demands, as a π acceptor, more electron density. The latter is moved from the carbonyls to phenanthroline. We will try to clarify this concept in terms of a fragment orbital analysis. First of all, starting from **1b**, we confirm that the σ donation of the diimine to the system reduces as we move towards **1**. This is also clearly demonstrated by the contributions of the W(CO)$_4$ empty orbitals to the formation of $27b_2$ (HOMO–5) and $35a_1$ (HOMO–8) orbitals (3.9% and 4.9% for **1b**, 3.8% and 4.6% for **1a** and **1**). The total donation is reduced from 0.398 to 0.394 and 0.385 e$^-$, respectively. On the other hand, back-donation to *o*-phenanthroline is increased when going from **1b** to **1a**, as expected. Back-bonding occurs through the transfer of electron density from the HOMO–2 of W(CO)$_4$ to the $5b_1$ and $6b_1$ of the diimine, forming the $13b_1$ and $14b_1$ orbitals of the complex. Thus,

the contribution of the empty orbitals of the diimine to the formation of $13b_1$ increases from 7.9% to 8.6%, while the contribution of the $W(CO)_4$ fragment to $5b_1$ of the diimine increases from 7.5% to 8.2%. Back-donation reduces slightly when going from **1a** to **1** and this is where the electron repulsion concept is applied. $W(CO)_4$ and phenanthroline filled orbitals repulse each other and the oxygen atoms bend in order for these forces to reach equilibrium. But this is rather the result than the cause (vide infra).

Up to this point we determined the nature of the driving forces that bend the system from **1b** to **1**, through **1a**. In summary, the major effect comes from the existence of phenanthroline. The system adopts the geometry that minimizes the electron repulsion for all the present ligands. This is further enhanced by the need for diminishing the electron repulsion of the fragment. If the system has a perfect octahedral geometry before these changes started to occur then another feature must also be explained. The bend of the axial carbonyls is sensitive to the back-bonding of the equatorial diimine ligands. Thus, the axial COs deviate from linearity by 3.25°, while the related differentiation in the case of the equatorial COs is only 1.35°. This means that the axial ligands are the most sensitive to the coordination diimines on the metal atom. The aforementioned conclusion is rather peculiar if the *trans* influence is kept in mind, along with the fact that the bite angle of the equatorial COs certainly has to be enlarged in order for the phenanthroline σ bonding to be effective. A natural arising question is why that happens. To provide a satisfactory answer we should examine the way back-donation evolves in space. As we have already mentioned back-bonding to phenanthroline is set through the $5d_{xz}$ orbital (b_1 in symmetry) of the metal and consequently the carbonyls that compete with the diimine are the axial and not the equatorial ones.

To proceed with our analysis, the bending of oxygen atoms should be further explained. As we have already mentioned, in the axial sites the carbonyls bend towards the "inside", while in the equatorial ones they bend towards the "outside". According to a frontier orbitals point of view, bending in the latter case causes stabilization of the orbitals centered on both carbonyls and the metal, whereas it destabilizes the diimine orbitals in a complete inverse way as compared to **1a**→**1**. Thus **1c**→**1** offers 0.86 kJ/mol to the system. This is slightly less than the 1.14 kJ/mol for **1a**→**1**. The induced stabilization, as an absolute value, is in both cases rather small. On the other hand, if compared to the relative value for **1b**→**1a**, which arises from changes in back-donation, it is considered relatively high and this finding becomes more valuable if we take into account the significantly smaller geometric change in this case.

Going from **1c** to **1** the back-donation to the carbonyls increases (0.3% rise in the carbonyl LUMO contribution to $36a_1$). This happens because carbonyls have a better overlap with the $5d_{x^2-y^2}$ of the metal, which is the most suitable d orbital for back-donation, because of its orthogonal arrangement to the *yz* plane. Furthermore, a linear combination of d_{z^2} and $d_{x^2-y^2}$ is also present. This situation leads us to reevaluate the C to O σ donation. In order to reevaluate this process we used the concept of natural hybrid orbitals, which are derived by a natural bond orbital analysis.[15] Before we proceed we have to clarify that although the absolute values, which are extracted from the NBO analysis, are different from those extracted through the Mulliken population analysis applied in the rest of this report, the following results and described trends are in total accordance. Indeed, σ bonding through the equatorial W–C–O unit is also favored. Calculated deviations between the geometrical direction of the bond and the related direction of the hybrid orbital are reduced by up to 1.9° for W–C and 4.7° for C–O. This is a direct consequence of the diimine ligation to the system.

The case of **1a**→**1** seems to be analogous. It is clear that axial carbonyls accept electron density from the metal d_{xy} orbital. Unfortunately, in each case changes in fragment contributions and relative energy are below the method precision. The hybrid orbitals of the complex seem to slightly change their conformation due to a best alignment of the carbon atoms to the π-orbital of the tungsten, at the expense of carbon–oxygen overlap and σ bonding.

Trying to summarize the above facts, we must emphasize that the suitable orbitals for back-donation are the d_{xz}, d_{xy}, and $d_{x^2-y^2}/d_{z^2}$ metal orbitals, which offer electron density to the diimine and also the axial and equatorial carbonyls. The bending of the C–O bonds is, in each case, the result of the tendency of the system to adopt a configuration in space that minimizes the electron repulsions between the bonds involved in the complex formation. The whole situation is best described by **1d**, which contains all the aforementioned changes. As demonstrated in Table 2 this structure shows the greatest destabilization, giving a final value of 2.95 kJ/mol. Despite the fact that this value is relatively low it is indicative of the energy stabilization that is offered to the system from the arrangement of the ligand in space, in such a way that is convenient from an electronic point of view.

2.2. Relation Between Structure, Back-Bonding, and Electron Properties

At the second level of our approach, we tried to discover the trends that govern the structural features of the complexes under study, such as the bending of axial carbonyls in terms of the ability of the ligand to partake in back-donation. As already mentioned (vide supra), these features are anticipated to be correlated to the electronic properties of the compound. This is an essential hypothesis, which we try to test in this report.

There are three important factors that govern the electronic structure of $W(CO)_4$(diimine) complexes. First of all, the σ-donating ability of the coordinating nitrogen atoms, followed by the existence of π*-orbitals of proper energy and symmetry, which are suitable for the evolution of back-donation, and thirdly the magnitude of the binding N–W–N angle. Taking all these factors into consideration we properly selected eight ligands in order to demonstrate probable induced differences in compound structure and

electronic behavior. First of all, we employed 1,10-phenanthroline (phen – compound **1**) and 2,2′-bipyridine (bpy – compound **2**), which are two of the most widely used aromatic ligands in synthesis. In order to test the influence of symmetry and binding angle we also employed two pyridine moieties (2py – compound **3**), in a sense that they would create an aromatic, but not a chelated first coordination sphere, around the metal. Consequently, we selected 1,4-diazabutadiene (DAB – compound **4**), *N*,*N*′-bis-methyl-1,4-diazabutadiene (Me-DAB – compound **5**) and *N*,*N*′-bis-isopropyl-1,4-diazabutadiene (*iPr*-DAB – compound **6**). These are highly symmetric aliphatic diimines and their properties will be compared to those of the aromatic ones. Finally, we introduced 1,2-ethylenediamine (en – compound **7**), since it is a bidentate diamine without any orbitals suitable for back-bonding and two ammonia ligands (2 NH_3 compound **8**) with almost the same σ-donating ability to the en, but without any steric constraints present.

Structural characteristics of compounds **2**–**8** are depicted in Table 4. Relative data for **1**, extracted from Table 1 and Table 2 (vide supra) are also reported for uniformity purposes. All data presented are extracted at the G98-B3LYP level of theory and show satisfactory agreement with other reported computational results and crystal structures.[4,9,11] To the best of our knowledge, compound **8** has not yet been prepared, but is included in our analysis for comparison purposes.

All of the complexes under study adopt a distorted pseudo-octahedral geometry. We started our analysis with the approximation described in all standard textbooks.[16] Within the framework of π* back-bonding different structures are compared based on the magnitude of the W–L and C–O bond lengths. In our case, the axial W–C bonds are significantly longer than the relative equatorial ones. The length of the W–N bond is increased in the order **4** < **5** ≈ **6** ≈ **2** < **1** < **3** < **8** < **7**. Thus, bonding of the N ligand seems to be stronger in the case of the DAB ligands as compared to the aromatic ones, while the amine complexes demonstrate weaker bonding along the series. This series is also indicative of the nitrogen hybridization where sp^3 hybridization (present in the amines) affords longer W–N bonds. The relative series, regarding the W–C_{eq}, W–C_{ax}, C–O_{eq}, and C–O_{ax} bonds, is **8** < **3** ≈ **1** ≈ **2** < **7** < **4** < **6** ≈ **5**, **8** ≈ **3** < **1** ≈ **2** < **4** ≈ **7** < **6** ≈ **5**, **5** < **6** < **7** < **4** < **3** ≈ **1** ≈ **2** ≈ **8**, and **5** ≈ **6** < **7** < **4** < **1** ≈ **2** < **3** ≈ **8**, respectively. According to the above bonding scheme we conclude that diazabutadiene ligands are better π* acids than *a*-diimines and amines, a finding that definitely make sense. Nevertheless, there are some points in the above series that certainly deserve to be further explained. First of all, within the R-DAB ligands it seems that the series of π* acidity that holds is H- < Me- < *iPr*-. In other words, the increase of the electron-releasing character of the substituents on the nitrogen atoms in the R-DAB ligands increases the electron-donating character of the σ bond and in consequence it increases the π-acceptor character. The observed trend is certainly not normally expected. Secondly, the first coordination sphere of **7** seems to resemble that of the R-DAB ligands, while several similarities exist between **3** and **8**. This trend should be further explained on the basis of important differences in nature between these organic substances.

To proceed with our analysis we examined, at first, a structural feature that is certainly underestimated in the existing literature in the field. This is the binding and bending angles of the carbonyl moieties. In Figure 3 and Figure 4 these features are schematically depicted. Thus, we observe that the N–W–N bite angle increases in the series **5** ≈ **4** ≈ **6** < **2** < **7** ≈ **1** < **3** ≈ **8**, while the relative series in the case of C_{eq}–W–C_{eq}/O_{eq}–W–O_{eq} (φ_1/φ_2) and C_{ax}–W–C_{ax}/O_{ax}–W–O_{ax} (φ_3/φ_4) is **8** < **3** ≈ **7** < **2** ≈ **1** < **6** < **5** < **4** and **4** < **6** <

Table 4. Comparison of selected calculated bond lengths [Å] and angles [°] for the ground-state structure of complexes **1**–**8** along with calculated data on electron density donation between the W(CO)$_4$ and the diimine fragments.

C	**1**	**2**	**3**	**4**	**5**	**6**	**7**	**8**
W–N	2.226	2.219	2.274	2.134	2.215	2.216	2.365	2.349
W–C_{ax}	2.033	2.033	2.023	2.042	2.068	2.064	2.049	2.023
W–C_{eq}	1.976	1.977	1.975	2.002	2.016	2.011	1.985	1.965
C–O_{ax}	1.187	1.187	1.191	1.183	1.158	1.162	1.169	1.192
C–O_{eq}	1.197	1.197	1.196	1.19	1.165	1.17	1.174	1.198
C=N	1.384	1.378	1.368	1.338	1.308	1.312	1.487	–
N–W–N	74.2	73.2	84.7	72.1	72	72.5	73.9	84.7
C_{ax}–W–C_{ax}	173.5	173.2	174.9	162.1	169.4	166.1	174.9	176.4
O_{ax}–W–O_{ax}	171.1	170.7	172.6	158.9	167	162.7	172.5	174.4
C_{eq}–W–C_{eq}	92.7	92.3	90.9	99.6	95.1	94.8	91.1	90.3
O_{eq}–W–O_{eq}	94.8	94.6	91.8	102.2	97.0	96.8	92.4	90.9
ΔE[a]	2.36	2.33	2.92	2.43	2.36	2.40	3.51	3.48
b[b]	0.385	0.391	0.460	0.427	0.464	0.574	0.472	0.477
bd[b]	0.022	0.021	0.021	0.121	0.111	0.091	0	–0.02
r[b]	–0.514	–0.536	–0.084	–0.517	–0.434	–0.46	–0.338	–0.41
Total π*(N) to H-2[c]	8.3[d]	8.8[e]	4.1[f]	30.3[g]	20.4	20.5	0	0

[a] HOMO–LUMO energy differece in eV. [b] Total charge donation, back-donation, and electron repulsion between W(CO)$_4$ and diimine fragments. [c] Mainly the HOMO–2 [W(CO)$_4$ – b_1 in symmetry] to b_1*-LUMO (N ligand) type. [d] It contains a 1.8% contribution from the LUMO+2 of the phen. [e] It contains a 2.8% contribution from the LUMO+1 of the bpy. [f] An interaction between the orbitals of a symmetry. [g] Contains 1.0% contribution from the LUMO+1 of DAB.

5 < **2** ≈ **1** < **7** ≈ **3** < **8**, respectively. All the complexes under study share the same structural features, described earlier (vide supra). The $W(CO)_4$ fragment deviates from orthogonality with the axial carbonyls bending away, while the equatorial ones bend towards the N ligand. In both cases, the bending of the oxygen atoms is larger. Moreover, several other features deserve attention. First of all, both axial and equatorial carbonyls deviate from orthogonality in an analogous way and the following relations, Equation (1) and (2), are extracted.

$$\varphi_1 = -0.5935\ \varphi_3 + 195.03\ (r = 0.97) \quad (1)$$

$$\varphi_2 = -0.6372\ \varphi_4 + 202.59\ (r = 0.95) \quad (2)$$

φ_1 and φ_2 are the angles C_{eq}–W–C_{eq} and O_{eq}–W–O_{eq} and φ_3 and φ_4 the angles C_{ax}–W–C_{ax} and O_{ax}–W–O_{ax}, respectively.

Moreover, as it is depicted in Figure 3 and Figure 4 in both cases the deviation from linearity observed in the carbonyl moiety is enhanced, in general terms, with the deviation of the whole group from orthogonality. Thus, in the case of the axial carbonyls, the largest deviation is observed for **6** and **4** and the smallest for **8** and **9**, whereas for the equatorial carbonyls the largest deviation is observed in **4** and the smallest are also in **8** and **9**. Last but not least, the trend followed within the $W(CO)_4$ moiety is reversed in the case of the W–heteroligand bite angle. Nevertheless, we

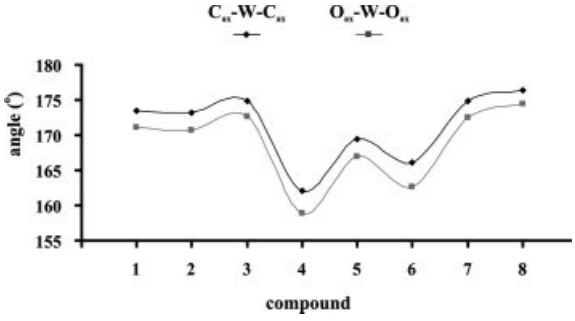

Figure 3. Schematic diagram of the C_{ax}–W–C_{ax} and O_{ax}–W–O_{ax} angles for compounds **1**–**8**.

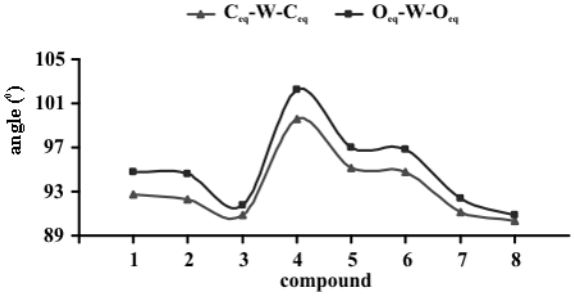

Figure 4. Schematic diagram of the C_{eq}–W–C_{eq} and O_{eq}–W–O_{eq} for compounds **1**–**8**.

should emphasize the fact that the two compounds without a bidentate ligand, namely **3** and **8**, show the same N–W–N angle, despite the different nature of the nitrogen ligands.

Proceeding with our discussion in electronic terms the contribution of different fragments to the frontier orbitals of the complexes is depicted in Table 5. Complex **2** has a framework of frontier orbitals analogous to the aforementioned one for **1** (vide supra), with the expected changes that arise from the fact that they have different aromatic diimine groups. For example, the first unoccupied diimine based a_2 orbital lies at a lower energy in **1** as compared to **2**. On the contrary in compounds **4**–**6** a different pattern is observed. The LUMO+3/+4 in **2** are stabilized and become the LUMO+1/+2 in **3**. These are predominantly axial carbonyl in character. The HOMO manifold for these compounds remains localized, mainly on the metal giving a relevant bonding scheme.

Complex **3** contains two pyridine moieties and not a bidentate ligand. The relaxed structure, in which the two pyridines are twisted from the planar disposition in order to minimize the hindrance that appears between the pyridine *ortho*-H atoms, destabilizes the frontier orbitals and affects the back-donation pathway. As a result back-bonding is no longer evolved through an orbital of b symmetry. In the case of pyridine ligands a metal $d_{x^2-y^2}/d_{z^2}$ (a_1 in C_{2v} first coordination sphere) linear combination interacts with a pyridine-based a* orbital (Figure 5).

Finally, in the case of the diamine and bis-amine complexes the bonding scheme, apart from the three highest occupied orbitals, is different. Most of the unoccupied orbitals are carbonyl localized, with the contribution of the heteroligand being of low to only moderate importance (e.g. LUMO+3 in **7** and LUMO+2 in **8**). Moreover, an unoccupied orbital with a predominant d(σ*) character was not found in any of the above compounds. In cases where this sort of contribution existed it corresponded to only a part of a highly delocalized orbital. Thus, low-lying LF states contradict the arguments of the traditional ligand field theory. This fact is consistent with previous work done by Vlček et al.[4]

In terms of back-donation to the N ligand the main pathway followed for all cases (apart from **3**) is the out-of-phase interaction between an orbital of d_{xz} tungsten/π*-axial carbonyl character and a π* heteroligand. This is best demonstrated by the HOMO–2 and LUMO (vide supra). Through an FMO analysis, analogous to that described in the previous paragraph, we concluded the following series of increasing back-donation, **8** ≈ **7** < **3** < **1** < **2** < **5** ≈ **6** < **4**, with the diamine and bis-amine compounds showing trivial back-bonding and **4**, which contains the DAB ligand, having the maximum back-bonding in the series. The comparison was based on the interaction of the HOMO–2 of the $W(CO)_4$ fragment (HOMO in the case of **3**) with the π* orbitals of the heteroligand (LUMO to LUMO+2 of proper symmetry), as demonstrated in Table 4. The same series in terms of the ligands is NH_3 ≈ en < py < bpy < phen < Me-DAB ≈ *iPr*-DAB < DAB. Thus, aliphatic diimines interact stronger with the metal fragment than aromatic ones,

Table 5. Contribution of different fragments to the valence orbitals of complexes **2**–**8**. The HOMO and LUMO are shown in bold.

MO	*E* [eV]	W	diimine	CO_{ax}	CO_{eq}
2					
$34a_1$	–1.22	16.0	–2.2	86.0	0.2
$26b_2$	–1.49	20.2	–0.2	70.8	9.1
$7a_2$	–1.97	0.1	97.8	0.5	1.6
$14b_1$	–2.12	1.0	96.8	1.0	1.2
$13b_1$	**–3.00**	**3.7**	**90.1**	**3.0**	**3.2**
$33a_1$	**–5.33**	**63.8**	**0.8**	**0.8**	**34.6**
$6a_2$	–5.61	58.3	3.8	22.8	15.1
$12b_1$	–5.64	54.7	13.6	21.6	10.1
$5a_2$	–7.83	0.1	99.9	0.0	0.0
$11b_1$	–9.19	1.2	95.3	3.0	0.5
$4a_2$	–9.20	1.4	97.5	0.8	0.3
3					
41b	–1.30	11.4	46.4	36.2	6.0
40b	–1.57	5.8	54.5	39.3	0.5
41a	–1.72	3.6	77.0	19.6	–0.2
40a	–2.18	2.6	89.8	2.8	4.8
39b	**–2.21**	**1.4**	**94.5**	**2.3**	**1.9**
39a	**–5.13**	**61.2**	**7.2**	**0.3**	**31.3**
38b	–5.56	60.1	3.1	25.0	11.8
38a	–5.58	60.2	1.3	23.9	14.5
37b	–8.28	0.1	99.8	0.1	0.0
37a	–8.39	0.2	99.5	0.1	0.2
36b	–8.99	0.8	95.3	1.9	2.1
4					
$12b_1$	–0.51	13.2	2.7	11.6	72.6
$16b_2$	–1.02	3.4	0.5	20.6	75.5
$23a_1$	–1.58	12.1	–0.6	85.7	2.9
$15b_2$	–1.93	16.9	0.7	70.1	12.3
$11b_1$	**–3.48**	**12.6**	**62.6**	**15.3**	**9.4**
$22a_1$	**–5.92**	**63.2**	**1.7**	**3.4**	**31.7**
$4a_2$	–6.22	54.7	6.8	21.8	16.7
$10b_1$	–6.35	43.0	34.1	18.7	4.2
$3a_2$	–9.47	4.6	92.8	1.9	0.8
$14b_2$	–10.13	3.0	70.3	2.4	24.3
$21a_1$	–10.28	4.8	74.2	1.9	19.1
5					
$13b_1$	–0.12	17.3	1.8	13.9	67.0
$19b_2$	–0.37	3.5	1.0	17.4	78.1
$26a_1$	–1.27	13.0	–0.4	86.7	0.7
$18b_2$	–1.59	17.8	1.3	72.1	8.7
$12b_1$	**–3.07**	**10.0**	**74.5**	**8.5**	**7.0**
$25a_1$	**–5.43**	**65.5**	**1.1**	**1.5**	**31.9**
$5a_2$	–5.76	59.3	4.0	21.9	14.8
$11b_1$	–5.91	51.4	23.2	18.9	6.5
$4a_2$	–8.65	2.3	96.7	0.8	0.2
$17b_2$	–9.36	3.0	81.7	1.1	14.3
$24a_1$	–9.68	5.1	80.1	1.2	13.5
6					
$17b_1$	–0.04	16.2	2.9	13.2	67.7
$23b_2$	–0.39	3.7	1.1	19.4	75.8
$30a_1$	–1.18	12.4	–0.5	87.0	1.1
$22b_2$	–1.51	17.4	1.3	71.1	10.2
$16b_1$	**–3.01**	**9.3**	**73.5**	**9.5**	**7.8**
$29a_1$	**–5.42**	**64.7**	**1.5**	**1.9**	**31.9**
$9a_2$	–5.70	57.5	5.5	21.7	15.4
$15b_1$	–5.84	50.4	23.5	19.8	6.2
$8a_2$	–8.42	3.2	95.2	1.2	0.4
$21b_2$	–8.77	1.5	88.5	1.0	9.0
$28a_1$	–9.13	4.1	89.0	0.7	6.1
7					
29b	0.35	33.2	16.2	0.3	50.4
28b	0.17	34.3	4.5	16.9	44.3
29a	0.09	62.8	24.0	16.5	–3.2
27b	0.01	37.9	8.9	28.7	24.5
28a	–1.31	20.8	8.2	71.1	–0.2
26b	**–1.52**	**25.8**	**6.8**	**60.9**	**6.5**
27a	**–5.03**	**65.3**	**0.8**	**0.5**	**33.4**
26a	–5.40	61.7	0.2	24.2	13.9
25b	–5.41	63.3	0.7	24.7	11.3
24b	–9.39	2.3	78.4	1.7	17.7
25a	–9.43	3.9	81.0	1.4	13.7
23b	–10.22	4.6	0.5	71.4	23.5
8					
50	–0.06	18.3	0.0	21.8	60.0
49	–0.29	30.3	7.5	25.4	36.8
48	–0.58	56.3	22.5	25.2	–4.0
47	–1.75	29.8	9.7	60.8	–0.2
46	**–1.80**	**24.9**	**5.1**	**63.9**	**6.1**
45	**–5.28**	**64.6**	**0.6**	**0.2**	**34.7**
44	–5.70	61.2	0.2	25.3	13.3
43	–5.72	61.4	0.4	24.8	13.4
42	–9.83	2.7	63.6	2.8	30.9
41	–10.09	3.5	60.4	4.1	31.9
40	–10.25	4.0	0.4	63.8	31.8

with the amines not showing back-donation at all. This conclusion certainly makes sense and it certainly reflects the nitrogen hybridization changing from sp^3 for NH_3 to sp^2 for DAB.

Taking the aforementioned findings into consideration we verified that the bond lengths do not demonstrate the correct behavior according to the induced back-donation. On the contrary, the C–W–C deviation from orthogonality and C–O deviation from linearity follow the back-donation trends! In other words, the stronger the back-donation the larger the deviations. This observation is originally presented in this report. Indeed, C–W–C and O–W–O angles correlate effectively with the observed back-donation magnitude (bd), as proven from the following relations [bd can also be provided as a function of the angles φ_1 and φ_2, through Equations (1) and (2) since the deviation of the equatorial ligands are a consequence of the bending of the axial ones]. In these relations bd is the total percentage of contribution of unoccupied π*-type heteroligand orbitals in the back-donation pathway.

From the above Equation (3) and (4) we verify that the bite angles of the CO groups are not only indicative of π* back-donation but they are also correlated to back-donation in a linear fashion. In other words, it is proved that the structural indices that best describe back-donation in symmetric compounds of the type W(CO)$_4$(NN) or W(CO)$_4$N$_2$, are the deviations of the C–W–C angles from orthogonality and O–C–W angles from linearity. The larger the existing deviation the stronger the back-donation. This contradicts the traditional concept of bond lengths, which does not always lead to correct results. This conclusion

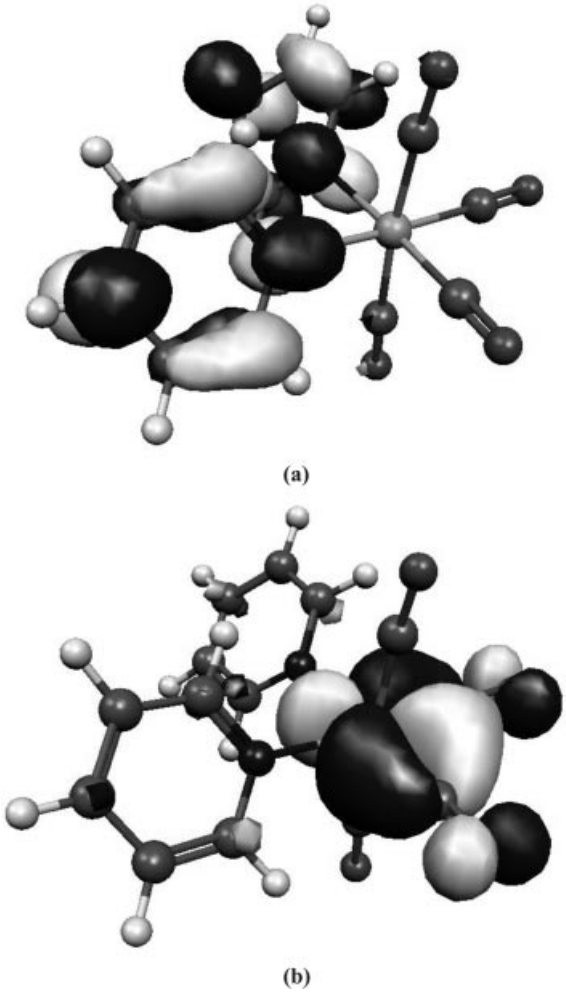

Figure 5. Contour plots of the HOMO (a) and LUMO (b) for compound **3**.

should also apply to the symmetric carbonyl compounds with other types of ligands, such as phosphanes and phosphites.

$$bd = -2.1238\ \varphi_3 + 375.51\ (r = 0.97) \quad (3)$$

$$bd = -1.9562\ \varphi_4 + 341.63\ (r = 0.97) \quad (4)$$

3. Concluding Remarks

In the present report, we tried to study the structures of $W(CO)_4(NN)$ and $W(CO)_4N_2$ compounds in terms of π* back-donation. Our approach was divided into two parts. Firstly, we proved, for the first time, that the observed structural deviations from orthogonality, regarding C–W–C bite angles and deviations from the linearity of the O–C–W angles present in complexes of this type, have their origin in the evolution of the necessary back-donation pathways. The energy difference between the two structures (the bent and the totally orthogonal one) is computed to be 2.95 kJ/mol.

Secondly, we analyzed the back-donation pathways of a series of compounds having different types of ligands. We proved that this is achieved through a $d_{xz} \rightarrow$ N-ligand electron donation, except in the case of the $W(CO)_4(py)_2$ compound. Moreover, we showed that back-donation is correlated to the above-mentioned structural features in a linear manner.

Keeping this scheme in mind, along with the fact that among all the ligands studied in our series DAB is involved in the maximum back-bonding and NH_3 the minimum, we can develop a new structure-to-properties type scale regarding back-donation. From a multiple regression analysis of the aforementioned data (Figure 6) we developed the following relation (details for the linear regression are supplied in the Supporting Information) which implies that the magnitude of back-donation is a linear combination of the four angles of the CO groups (since φ_1 and φ_2 are dependant on φ_3 and φ_4, respectively), see Equation (5).

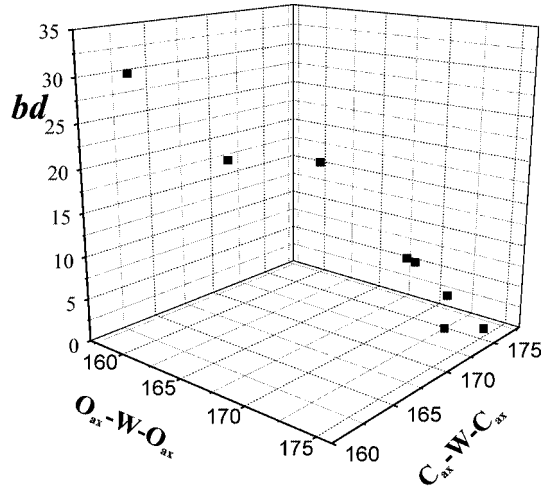

Figure 6. Scatter plot of bd = $f(\varphi_3, \varphi_4)$. $R^2 = 0.98$ (from multiple regression analysis).

$$bd = 510.15 - 10.58\ \varphi_3 + 7.79\ \varphi_4 \quad (5)$$

The standard deviation is 2.34.

Moreover, if we define the π* acidity related to the DAB (100% π* acid) and ammonia molecules (0% π* acid) we get Equation (6).

$$bd' = 3.00\ bd \quad (6)$$

On the basis of Equation (6) we can attribute a 29% of π*-accepting ability to bpy compared with DAB.

The extent of back-donation and thus the bending of the $W(CO)_4$ group should be correlated to other properties of the system such as the slope of solvatochromic plots.[8] It is well known that the complexes under study exhibit a large negative solvatochromism, which refers to the blue shift of the low energy MLCT transition of the complex, with a simultaneous increase in the polarity of the solvent. This phenomenon is directly related to a difference between the ground- and excited-state dipole moment. The ground-state dipole moment is certainly determined by the geometry of the compounds and this geometry has its origin in the extent of back-donation as we have already proved (vide infra). As a result the extent of solvatochromism should be correlated to the extent of back-donation.

4. Computational Details

Ground-state electronic structure calculations of all complexes under study have been performed using density functional theory (DFT)[17] methods by employing the Gaussian 98 software package.[18] The functional that was used throughout this study is the B3LYP, consisting of a hybrid exchange functional, as defined by Becke's three-parameter equation[19] and the Lee–Yang–Par correlation functional.[20] The ground-state geometries were obtained in the gas phase by full geometry optimization and the optimum structures, located as stationary points on the potential energy surfaces, were verified by the absence of imaginary frequencies. Moreover, the derived wave functions were free from internal instabilities. Structures were regularized in order to satisfy the C_{2v} geometry in **1**–**2** and **4**–**6**. Complex **3** was optimized under no symmetry constraint. The optimum structure obtained a practically C_2 symmetry and the optimization was repeated in this point group. Complex **7** was optimized also under the C_2 symmetry, whereas complex **8** was optimized without any symmetry constraint. The basis set used throughout this study is the full double-ζ LANL2DZ basis function, together with the corresponding effective core potential for tungsten.[21] Percentage compositions of molecular orbitals from the four contributing fragments (the metal, the N ligand, the axial and equatorial carbonyls) were calculated and analyzed using the AOMix and AOMix-CDA programs, with the latter being extensively used for the fragment molecular orbital (FMO) analysis.[22] The graphics presented here were drawn with the aid of Molekel.[23] An NBO population analysis has been performed with the NBO 3.1 program as implemented in Gaussian.[15b] Finally, a multiple regression analysis was carried out using the commercial Origin 6.0 software package.

Supporting Information (see also the footnote on the first page of this article): Mulliken charges for compounds **1** and **1a**–**1d** (Table S1), details for the linear regression provided for Equation (5) and calculated atomic coordinates (S2–S9) for all compounds under study.

Acknowledgments

The project was cofunded by the European Social Fund (EPEAEK II)and National Resources (PYTHAGORAS).

[1] A. Vlček Jr., *Coord. Chem. Rev.* **2002**, *230*, 225–242.
[2] A. J. Lees, *Coord. Chem. Rev.* **1998**, *177*, 3–35.
[3] D. J. Stufkens, *Coord. Chem. Rev.* **1990**, *104*, 39–112.
[4] a) S. Záliš, M. Busby, T. Kotrba, P. Matousek, M. Towrie, A. Vlček Jr., *Inorg. Chem.* **2004**, *43*, 1723–1734; b) S. Záliš, I. R. Farrel, A. Vlček Jr., *J. Am. Chem. Soc.* **2003**, *125*, 4580–4592; c) I. R. Farrel, J. van Slageren, S. Záliš, A. Vlček Jr., *Inorg. Chim. Acta* **2001**, *315*, 44–52; d) I. R. Farrel, H. František, S. Záliš, T. Mahabiersing, A. Vlček Jr., *J. Chem. Soc., Dalton Trans.* **2000**, 4323–4331; e) S. Záliš, C. Daniel, A. Vlček Jr., *J. Chem. Soc., Dalton Trans.* **1999**, 3081–3086; f) S. Záliš, A. Vlček Jr., C. Daniel, *Collect. Czech. Chem. Commun.* **2003**, *68*, 89–104; g) Z. Hu, R. J. Boyd, H. Nakatsuji, *J. Am. Chem. Soc.* **2002**, *124*, 2664–2671.
[5] I. Veroni, C. Makedonas, A. Rontoyanni, C. A. Mitsopoulou, *J. Organomet. Chem.* **2006**, *691*, 267–281.
[6] a) D. R. Van Staveren, N. Metzler-Nolte, *Chem. Commun.* **2002**, 1406–1407; b) N. Metzler-Nolte, *Angew. Chem. Int. Ed.* **2001**, *40*, 1040–1043.
[7] V. Balzani, A. Juris, M. Venturi, S. Campagna, S. Serroni, *Chem. Rev.* **1996**, *96*, 759–833.
[8] I. Veroni, A. Rontoyanni, C. A. Mitsopoulou, *Dalton Trans.* **2003**, 255–260.
[9] a) H. J. B. Slot, N. W. Murral, A. Welch, *Acta Crystallogr., Sect. C* **1985**, *41*, 1309–1312; b) P. N. W. Baxter, J. A. Connor, J. D. Wallis, D. C. Povey, *J. Organomet. Chem.* **1992**, *426*, 187–194; c) M. A. Bakar, H.-K. Fun, K. Chinnakali, S.-G. Teoh, O. B. Shawkataly, F. M. Lopez, *Acta Crystallogr., Sect. C* **1993**, *49*, 582–584; d) E. C. Alyea, G. Ferguson, V. K. Jain, *Acta Crystallogr., Sect. C* **1994**, *50*, 854–857; e) R. S. Herrick, K. L. Houde, J. S. McDowell, L. P. Kiczek, G. Bonavia, *J. Organomet. Chem.* **1999**, *589*, 29–37; f) R. S. Herrick, C. J. Ziegler, H. Bohan, M. Corey, M. Eskander, J. Giguere, N. McMicken, I. E. Wrona, *J. Organomet. Chem.* **2003**, *687*, 178–184; g) H. tom Dieck, T. Mack, K. Peters, H.-G. von Schnering, *Z. Naturforsch., Teil B* **1983**, *38*, 568–579; h) J. Powell, A. Lough, M. Raso, *J. Chem. Soc., Dalton Trans.* **1994**, 1571–1576.
[10] a) H. Jinshuan, C. Qingrong, W. Manfrag, L. Shimei, *Chin. J. Struct. Chem.* **1985**, *4*, 69–71; b) H. Jinshuan, C. Qingrong, W. Manfrag, H. Meiyun, *Chin. J. Struct. Chem.* **1985**, *4*, 66; c) N. S. Magomedova, G. K.-I. Magomedov, *Metalloorg. Khim.* **1990**, *3*, 129–134.
[11] Q. Ye, Q. Wu, H. Zhao, Y.-M. Song, X. Xue, R.-G. Xiong, S.-M. Pang, G.-H. Lee, *J. Organomet. Chem.* **2005**, *690*, 286–290.
[12] M. H. B. Stiddard, *J. Chem. Soc.* **1962**, 4712–4715.
[13] A. Rosa, E. J. Baerends, S. J. A. van Gisbergen, E. van Lenthe, J. A. Goeneveld, J. G. Snijders, *J. Am. Chem. Soc.* **1999**, *121*, 10356–10365.
[14] a) S. Dapprich, G. Frenking, *J. Chem. Phys.* **1995**, *99*, 9352–9362; b) G. Frenking, N. Fröhlich, *Chem. Rev.* **2000**, *100*, 717–774.
[15] a) A. E. Reed, L. A. Curtiss, F. Weinhold, *Chem. Rev.* **1988**, *88*, 899–926; b) E. D. Glendening, A. E. Reed, J. E. Carpenter, F. Weinhold, *NBO Version 3.1*.
[16] F. A. Cotton, G. Wilkinson, *Advanced Inorganic Chemistry*, 5th ed., John Wiley & Sons, New York, **1988**.
[17] R. G. Parr, W. Yang, *Density Functional Theory of Atoms and Molecules*; Oxford University Press: Oxford, **1989**.
[18] , M. J. Frisch, G. W. Trucks, H. B. Schlegel, G. E. Scuseria, M. A. Robb, J. R. Cheeseman, V. G. Zakrzewski, J. A. Montgomery Jr., R. E. Stratmann, J. C. Burant, S. Dapprich, J. M. Millam, A. D. Daniels, K. N. Kudin, M. C. Strain, O. Farkas, J. Tomasi, V. Barone, M. Cossi, R. Cammi, B. Mennucci, C. Pomelli, C. Adamo, S. Clifford, J. Ochterski, G. A. Petersson, P. Y. Ayala, Q. Cui, K. Morokuma, D. K. Malick, A. D. Rabuck, K. Raghavachari, J. B. Foresman, J. Cioslowski, J. V. Ortiz, A. G. Baboul, B. B. Stefanov, G. Liu, A. Liashenko, P. Piskorz, I. Komaromi, R. Gomperts, R. L. Martin, D. J. Fox, T. Keith, M. A. Al-Laham, C. Y. Peng, A. Nanayakkara, M. Challacombe, P. M. W. Gill, B. Johnson, W. Chen, M. W. Wong, J. L. Andres, C. Gonzalez, M. Head-Gordon, E. S. Replogle, and J. A. Pople, *Gaussian 98, Revision A.9*, Gaussian, Inc., Pittsburgh PA, **1998**.
[19] A. D. Becke, *J. Chem. Phys.* **1993**, *98*, 5648–5652.
[20] C. Lee, W. Yang, R. G. Parr, *Phys. Rev. B* **1988**, *37*, 785–789.
[21] a) T. H. Dunning Jr., P. J. Hay, in: *Modern Theoretical Chemistry* (Ed.: H. F.Schaefer III); Plenum Press: New York, **1976**, vol. 3; b) P. J. Hay, W. R. Wadt, *J. Chem. Phys.* **1985**, *82*, 270–283.
[22] a) S. I. Gorelsky, *AOMix Progam, Revision 5.95 and AOMix-CDA, Revision 1.7*, http://www.sg-chem.net/; b) S. I. Gorelsky, A. B. P. Lever, *J. Organomet. Chem.* **2001**, *635*, 187–196.
[23] P. Flükiger, H. P. Lüthi, S. Portman, J. Weber, *MOLEKEL Version 4.3*, Swiss Center for Scientific Computing, Manno, Switzerland, **2000**–**2002**.

Received: July 18, 2006
Published Online: November 6, 2006

